



TECHNICAL UNIVERSITY OF CLUJ-NAPOCA

ACTA TECHNICA NAPOCENSIS

Series: Applied Mathematics, Mechanics, and Engineering
Vol. 66, Issue I, March, 2023

COMPARATIVE EVALUATION OF THE DYNAMIC BEHAVIOR OF TIRES EQUIPPING FORMULA STUDENT VEHICLES USING MATHEMATICAL MODELLING

Constantin-Cosmin DANCI, Irina DUMA, Thomas Imre Cyrille BUIDIN,
Nicolae CORDOȘ, Adrian TODORUȚ

Abstract: The paper captures studies regarding the wheel-track interaction, by modelling the contact patch of tires, in the case of the ART TU Cluj-Napoca Formula Student Team's racing car. The road conditions were considered according to the Skidpad circuit of the SAE competition and different inflation pressures were considered for the studied tires. Thus, by developing a numerical model in MATLAB software, with the help of which comparative results are obtained, and graphically analyzed, it is possible to identify the influences generated by the different considered tires on the dynamic behavior of the studied vehicle.

Key words: vehicle, tire, mathematical modelling, slip angle, lateral force, handling, stability

1. INTRODUCTION

Formula Student, a competition developed by SAE (Society of Automotive Engineers), is a global student community whose aim is to encourage students from all technical fields to put into practice the knowledge they have acquired during their years of study by designing and manufacturing a Formula Student racing car, which they will then use to compete in certain annual competitions. A competition is divided into static and dynamic events. Static events include project presentation, financial efficiency, and design report, while the dynamic events include acceleration competitions, Skidpad, a fast lap and endurance with a focus on energetic efficiency. A Formula Student car can be seen as a student version of a Formula 1 car, but one that is designed and manufactured by university students in accordance with competition regulations [9, 10, 11, 15, 16].

Tires play a key role in the dynamics of the vehicle, providing the link between the road and the vehicle, thus taking up the

forces and moments generated around the contact patch. For this reason, it is important to know the forces generated by the wheel in order to significantly improve vehicle handling, as well as to enhance ride comfort and occupant safety by allowing prediction of the travel trajectory [4, 5, 12, 13, 14, 20].

Figure 1 [13, 19] highlights the axis system representing the positive directions of the forces and moments, and the slip angle α formed between the wheel's median plane and the travelling direction. The forces generated during vehicle motion are with reference to the longitudinal force F_x , the lateral force F_y , the normal force F_z , and the moments encountered are with reference to the roll moment M_x , the pitch moment M_y and the alignment moment M_z [2, 13, 19].

The lateral forces acting on tires and the side slip angle are essential data for improving driving safety, handling, comfort, and dynamic performance of vehicles. Lateral force occurs when the vehicle enters corners, generating a side slip angle. Under normal driving conditions (low slip angle), a vehicle responds predictably to driver input. As the vehicle approaches its

handling limits, for example during an emergency avoidance maneuver or when a vehicle is subject to strong acceleration, a higher slip angle occurs and the dynamics of the vehicle become non-linear, making its response less predictable and potentially extremely dangerous [3, 4, 6, 8, 18, 20].

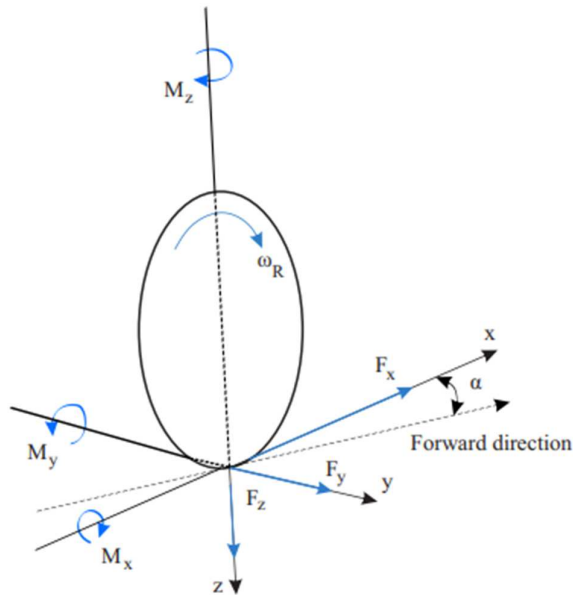


Fig. 1. Forces and moments acting on the wheel of a moving vehicle [13, 19].

In recent years, due to the non-linearity of tire behavior, considerable efforts have been made on vehicle control to improve safety and handling. To avoid the high costs of dynamic testing of tires on stands, various empirical tire models have been developed to describe the dynamic behavior of tires. It is recognized that these tire models fail to describe satisfactorily the behavior of tires in extreme scenarios, such as motorsport, where temperature and slip characteristics are significantly different and often very changeable. However, standard empirical models in the automotive industry can predict with relatively good accuracy important tire forces over a short range of vehicle operating conditions, and empirical tire models, such as the Magic Formula, play an essential role in research, control, and simulation studies of vehicle dynamics [1, 3, 5, 6, 12, 14, 17, 20, 21].

In Formula Student competitions, great attention is paid to the generation of lateral forces at wheel-road contact in the Skidpad event, where the circuit (Fig. 2) is made up of two tangent circles on the outside, where the main aim is to achieve the maximum possible lateral acceleration of the vehicle [22].

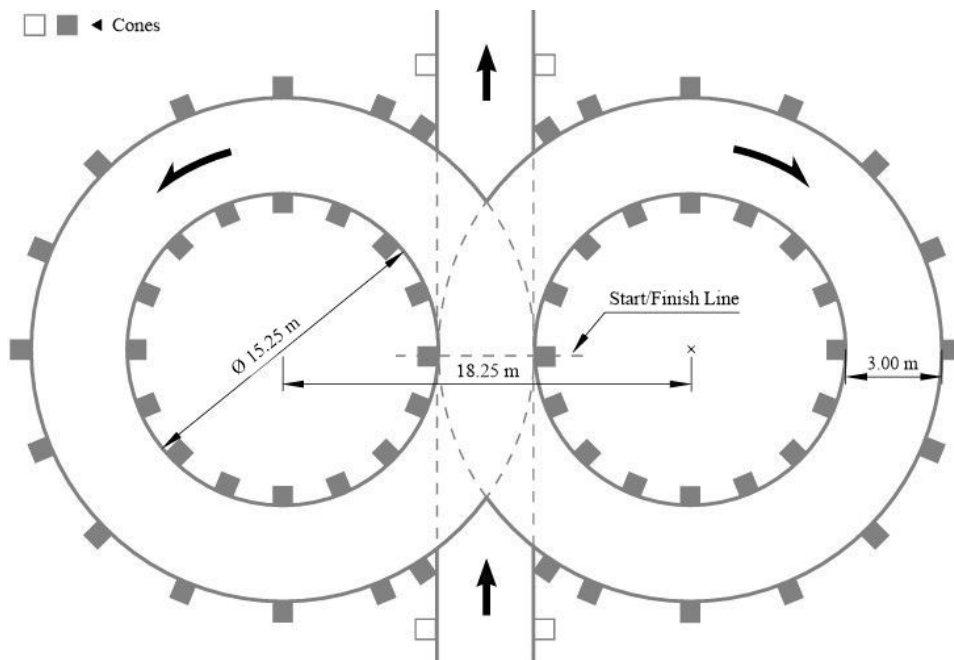


Fig. 2. Skidpad circuit layout [22].

In order to achieve the best dynamic performance from the car, Formula Student teams select a single tire type to use for their project. Teams must make an informed selection of race tires by comparing the mechanical properties of different tires provided by the “*Formula SAE Tire Test Consortium (FSAE TTC)*” and the “*Calspan Tire Research Facility (TIRF)*”, analyzing different influencing characteristic parameters such as pressure, camber angle, vertical loads, and temperature [5, 7, 11, 16, 18].

The aim of this work is to evaluate the influence of the inflation pressure of three types of tires developed by different manufacturers, compatible with the racing car of the *ART TU Cluj-Napoca, Formula Student Team*.

2. THE MAGIC FORMULA MODEL FOR TIRE MODELLING IN CURVES

The Magic Formula model has an empirical nature, and the modeling of curve behavior for the estimation of lateral force comprises a set of unitless parameters p and r , as well as a set of scaling factors λ . It is described by the relation [6, 13]:

$$F_y = G_{yk} \cdot F_{y0} + S_{Vyk}, \text{ in N,} \quad (1)$$

in which: G_{yk} is the weighting function, given by the relation [13]:

$$G_{yk} = \cos \left[C_{yk} \arctg \left\{ B_{yk} \kappa_s - E_{yk} (B_{yk} \kappa_s - \arctg(B_{yk} \kappa_s)) \right\} \right] / G_{yk0} (> 0), \quad (2)$$

where: C_{yk} is the coefficient that controls the level of horizontal asymptote; E_{yk} - curvature factor; B_{yk} - factor that influences the shape of the peak of the weighting function, given by the relation [13]:

$$C_{yk} = r_{Cy1}, \quad (3)$$

$$E_{yk} = r_{Ey1} + r_{Ey2} df_z, \quad (4)$$

$$B_{yk} = r_{By1} \cos[\arctg\{r_{By2}(\alpha^* - r_{By3})\}] \cdot \lambda_{yk}. \quad (5)$$

To avoid using the slip angle α (in radians) as an input quantity for large slip angles, it is recommended to use the slip angle tangent defined by the relation [13]:

$$\alpha^* = \operatorname{tg} \alpha \cdot \operatorname{sgn} V_{cx} = -\frac{V_{cy}}{|V_{cx}|}, \text{ in rad} \quad (6)$$

where: V_{cx} and V_{cy} are the components of the velocity vector V_c at the center of the contact patch, of the wheel [13]:

$$V_{cx} = V_c \cos \alpha, \text{ in m/s,} \quad (7)$$

$$V_{cy} = V_c \sin \alpha, \text{ in m/s.} \quad (8)$$

The velocity at the center of the contact patch shall be taken to be approximately equal to the forward velocity V_x of the vehicle, thus [13]:

$$V_x = V \cdot r_e, \quad (9)$$

in which: V is the velocity of the vehicle, in m/s; r_e - the rolling radius of the wheel, in m.

The notation df_z refers to the dimensionless increase of the vertical load F_z in relation to the nominal (adapted) load F'_{Z0} , by the relation [13]:

$$df_z = \frac{F_z - F'_{Z0}}{F'_{Z0}}. \quad (10)$$

Moreover, κ_s takes into account the sum of the longitudinal slip ratio κ and the horizontal displacement S_{Hyk} , by the relation [13]:

$$\kappa_s = \kappa + S_{Hyk}, \quad (11)$$

$$\kappa = -\frac{V_{sx}}{|V_{cx}|}, \quad (12)$$

$$S_{Hyk} = r_{Hy1} + r_{Hy2} df_z. \quad (13)$$

The notations V_{sx} and V_{sy} represent the components of the slip velocity vector V_s , referring to the longitudinal and lateral slip velocity respectively [13]:

$$V_{sx} = V_x - r_e \Omega, \text{ in m/s,} \quad (14)$$

$$V_{sy} = -V_{cx} \cdot \operatorname{tg}(\alpha), \text{ in m/s.} \quad (15)$$

The S_{Vyk} quantity is the vertical displacement, defined by the relation [13]:

$$S_{Vyk} = D_{Vyk} \sin[r_{Vy5} \arctg(r_{Vy6} \kappa)], \quad (16)$$

in which the peak factor D_{Vyk} depends on the angle of repose and the slip angle, thus [13]:

$$D_{Vyk} = \mu_y F_z \cdot (r_{Vy1} + r_{Vy2} df_z + r_{Vy3} \gamma^*) \cdot \cos[\arctg(r_{Vy4} \alpha^*)] \cdot \zeta_2. \quad (17)$$

The rotation due to the camber angle is considered by the relation [13]:

$$\gamma^* = \sin \gamma, \text{ in rad} \quad (18)$$

where μ_y is the coefficient of friction, given by the relation [13],

$$\mu_y = (p_{Dy1} + p_{Dy2} df_z) \cdot (1 - p_{Dy3} \gamma^{*2}) \cdot \lambda_{\mu y} / (1 + \lambda_{\mu V} V_s / V_0) (> 0). \quad (19)$$

The G_{yk0} factor is described by the relation [14]:

$$G_{y\kappa 0} = \cos \left[C_{y\kappa} \arctg \left\{ B_{y\kappa} S_{Hy\kappa} - E_{y\kappa} \left(B_{y\kappa} S_{Hy\kappa} - \arctg(B_{y\kappa} S_{Hy\kappa}) \right) \right\} \right]. \quad (20)$$

For normally encountered situations, where slip in turns can be neglected and the slope remains small, the factors ζ_i appearing in the equations can be set equal to unity [13]:

$$\zeta_i = 1 \quad (i = 0, 1, \dots, 8).$$

The notation F_{y0} refers to the lateral force under pure slip conditions, in which case the longitudinal slip ratio κ is considered to be zero and the relation used is [13]:

$$F_{y0} = D_y \sin \left[C_y \arctg \left\{ B_y \alpha_y - E_y \left(B_y \alpha_y - \arctg(B_y \alpha_y) \right) \right\} \right] + S_{Vy}, \quad \text{in N}, \quad (21)$$

which includes a series of parameters called *coefficients of the Magic Formula* described by the expressions B_y , C_y , D_y și E_y . Also, the variable α_y is the sum of the tangent of the lateral slip angle and the vertical translation coefficient S_{Hy} . Thus, the parameters are described by the relations [6, 13]:

$$\alpha_y = \alpha^* + S_{Hy}, \quad (22)$$

$$S_{Hy} = (p_{Hy1} + p_{Hy2} df_z) \cdot \lambda_{Hy} + p_{Hy3} \gamma^* \cdot \lambda_{Ky\gamma} \cdot \zeta_0 + \zeta_4 - 1. \quad (23)$$

The D_y notation refers to a peak coefficient [6, 13],

$$D_y = \mu_y \cdot F_z \cdot \zeta_2, \quad (24)$$

in which: μ_y is the friction coefficient; F_z - vertical load on the wheel, in N.

C_y refers to the shape coefficient of the model [6, 13]:

$$C_y = p_{Cy1} \cdot \lambda_{Cy} (> 0). \quad (25)$$

The variable E_y represents a curvature factor, defined by the relation [6, 13]:

$$E_y = (p_{Ey1} + p_{Ey2} df_z) \cdot \left\{ 1 - (p_{Ey3} + p_{Ey4} \gamma^*) \cdot \text{sgn}(\alpha_y) \right\} \cdot \lambda_{Ey} (\leq 1). \quad (26)$$

The B_y factor is the coefficient of elasticity in the transmission of lateral forces, defined by the relation [6, 13]:

$$B_y = K_{y\alpha} / (C_y D_y + \varepsilon_y), \quad (27)$$

where: $K_{y\alpha}$ the slope in the center of the curve; ε_y - additional quantity of reduced value (0.1) [13],

$$K_{y\alpha} = K_{y\alpha 0} \cdot (1 - p_{Ky3} \gamma^{*2}) \cdot \zeta_3, \quad (28)$$

in which $K_{y\alpha 0}$ is [13]:

$$K_{y\alpha 0} = p_{Ky1} F'_{z0} \sin \left[2 \arctg \left\{ F_z / (p_{Ky2} F'_{z0}) \right\} \right] \cdot \lambda_{Ky\alpha}. \quad (29)$$

Then, in relation (21) it is found S_{Vy} , which refers to the vertical translation coefficient [6, 13],

$$S_{Vy} = F_z \cdot \left\{ (p_{Vy1} + p_{Vy2} df_z) \cdot \lambda_{Vy} + (p_{Vy3} + p_{Vy4} df_z) \gamma^* \cdot \lambda_{Ky\gamma} \right\} \cdot \lambda'_{\mu y} \cdot \zeta_2, \quad (30)$$

and $\lambda'_{\mu y}$ is a special factor for degressive friction [13]:

$$\lambda'_{\mu y} = A_\mu \lambda_{\mu y} / \{ 1 + (A_\mu - 1) \lambda_{\mu y} \}, \quad (31)$$

where $A_\mu = 10$ [14].

3. OBTAINED RESULTS

Comparative analysis of tires at 0.068 MPa pressure (Fig. 3). Among 182.88/41.667R13 tires, the highest value of lateral force of 1906 N is found at the maximum value of side slip angle, while the maximum value of lateral force of 2451 N for 205/47R13 tires is found at -0.13 rad, and among 177.8/53.6R13 tires, the high values of lateral forces are in the range -0.055÷-0.081 rad, where the maximum value is the lateral force of 2285 N. At the same time, at the level of the graphical representation, it is noted that 177.8/53.6R13 tires have a higher lateral stiffness than 182.88/41.667R13 tires.

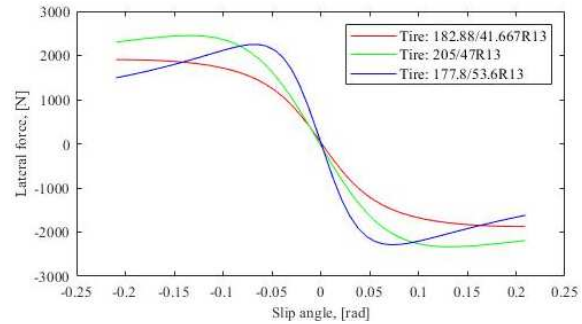


Fig. 3. Comparative analysis of tires at 0.068 MPa.

Comparative analysis of tires at 0.082 MPa (Fig. 4). Increasing tire inflation pressure causes a decrease in lateral force. The maximum values of lateral forces for the same lateral slip angles analyzed previously (within the studied range) are: 1879 N for 182.88/41.667R13 tires; 2379 N for 205/47R13 tires; 2113 N for 177.8/53.6R13 tires.

Comparative analysis of tires at 0.096 MPa (Fig. 5). The maximum lateral forces, for the same values of lateral slip angles analyzed previously (within the studied range) are:

1693 N for 182.88/41.667R13 tires; 2327 N for 205/47R13 tires; 1978 N for 177.8/53.6R13 tires.

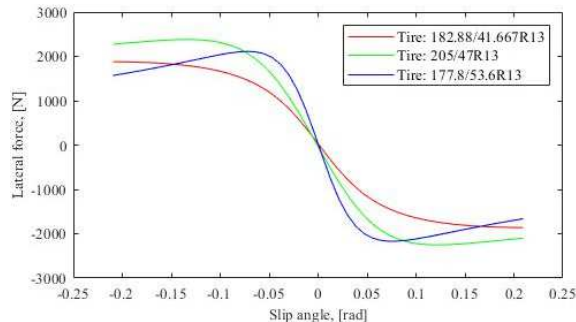


Fig. 4. Comparative analysis of tires at 0.082 MPa.

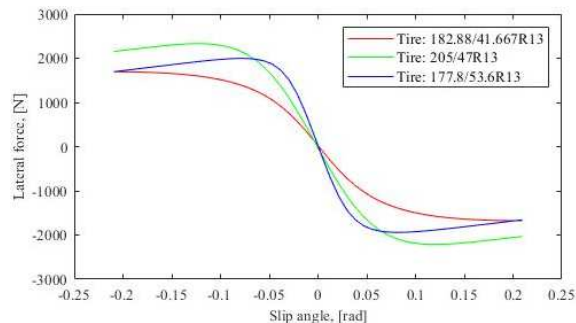


Fig. 5. Comparative analysis of tires at 0.096 MPa.

4. CONCLUSIONS

Based on the proposed objective, the wheel-track interaction analysis was carried out for three types of vehicle-specific tires for Formula Student, looking in detail at the influences of lateral forces generated by them on the car during the drive on the Skidpad circuit. Thus, the set of equations developing the magic formula model for tire modelling and simulation was implemented in the MATLAB software, and then the values of the experimental tire parameters provided by "Formula SAE Tire Test Consortium (FSAE TTC)" and "Calspan Tire Research Facility (TIRF)" were introduced for different values of inflation pressure.

Studies of tires 182.88/41.667R13, 177.8/53.6R13 and 205/47R13 revealed the following:

- 182.88/41.667R13 tires are stable and easily predictable for the pilot, because when the maximum side slip angle is reached, this type of tire ensures stability and

maneuverability as well as maintaining a constant maximum lateral force and lateral acceleration;

- 177.8/53.6R13 tires provide higher lateral forces than 182.88/41.667R13 tires, but the Formula Student car fitted with this type of tire is more difficult to control, as there is a risk of loss of stability at high side slip angles;
- 205/47R13 tires manage to significantly improve the stability and handling of the vehicle, as well as allowing the vehicle to travel at high speeds during cornering in the presence of these high lateral forces, while there is a much smoother transition of lateral force increase with increasing slip angle.

Following a comparative analysis of the analyzed tires (Fig. 6), the following aspects were noted:

- high values of lateral forces are found among tires with a pressure of 0.068 MPa, and this is justified by the fact that a low tire inflation pressure causes the contact patch to increase;

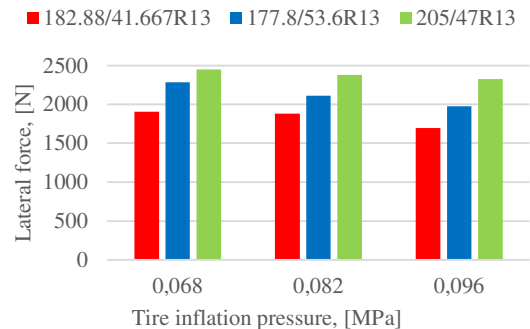


Fig. 6. Comparative analysis of tires.

- at an inflation pressure of 0.068 MPa, 205/47R13 tires have a maximum sidewall force 6.8% higher than those generated by 177.8/53.6R13 tires and 22.2% higher than the maximum sidewall force of 182.88/41.667R13 tires;
- at an inflation pressure of 0.082 MPa, 205/47R13 tires were found to produce 11.2% more maximum lateral force than 177.8/53.6R13 tires and 21% more than the

maximum lateral force of 182.88/41.667R13 tires;

- for the inflation pressure of 0.096 MPa, it was noted that 205/47R13 tires generate 15% more maximum lateral force than 177.8/53.6R13 tires and 27.2% more than 182.88/41.667R13 tires.

5. ACKNOWLEDGEMENT

The authors would like to thank “Formula SAE Tire Test Consortium (FSAE TTC)” and the “Calspan Tire Research Facility (TIRF)” for supporting us and providing the requisite information.

6. REFERENCES

- [1] Baffet, G.; Charara, A.; Stephant, J., *Sideslip angle, lateral tire force and road friction estimation in simulations and experiments*. Proceedings of the IEEE International Conference on Control Applications, October 2006, Pages 903-908, <https://doi.org/10.1109/CACSD-CCA-ISIC.2006.4776765>.
- [2] Balkwill, J., *Performance Vehicle Dynamics: Engineering and Applications*. Oxford, Butterworth-Heinemann, Elsevier Inc., 2018.
- [3] Doumiati, M.; Victorino, A.C.; Charara, A.; Lechner, D., *Onboard real-time estimation of vehicle lateral tire-road forces and sideslip angle*. IEEE/ASME Transactions on Mechatronics, Volume 16, Pages 601-614, August 2011, ISSN: 1083-4435, <https://doi.org/10.1109/TMECH.2010.2048118>.
- [4] Du, H.; Zhang, N.; Dong, G., *Stabilizing vehicle lateral dynamics with considerations of parameter uncertainties and control saturation through robust yaw control*. IEEE Transactions on Vehicular Technology, Volume 59, Pages 2593-2597, June 2010, ISSN: 0018-9545, <https://doi.org/10.1109/TVT.2010.2045520>.
- [5] Dye, J.; Lankarani, H., *Hybrid simulation of a dynamic multibody vehicle suspension system using neural network modeling fit of tire data*. Proceedings of the ASME Design Engineering Technical Conference, Volume 6, August 2016, American Society of Mechanical Engineers (ASME), <https://doi.org/10.1115/DETC201660435>.
- [6] Gaiginschi, R.; Drosescu, R.; Rakoși, E.; Sachelarie, A.; Filip, I.; Pintilei, M., *Siguranța circulației rutiere, Vol. I*. București, Editura Tehnică, 2004.
- [7] Harsh, D.; Shyrokau, B., *Tire model with temperature effects for formula SAE vehicle*. Applied Sciences (Switzerland), Volume 9, December 2019, ISSN: 2076-3417, MDPI AG, <https://doi.org/10.30/app9245328>.
- [8] Karnopp, D., *Vehicle Dynamics, Stability, and Control*, Second Edition. Boca Raton, CRC Press, Taylor & Francis Group, LLC, 2013.
- [9] Kaushal, R.; Chauhan, P.; Sah, Katya; Chawla, V.K., *Design and analysis of wheel assembly and anti-roll bar formula SAE vehicle*. Materials Today: Proceedings, Volume 43, Pages 169-174, 2020, ISSN 2214-7853, Elsevier Ltd, <https://doi.org/10.1016/j.matpr.2020.11.610>.
- [10] Kumar, Y.; Siddiqui R.A.; Upadhyay, Y.; et al., *Kinematic and Structural Analysis of Independent type suspension system with Anti-Roll bar for Formula Student Vehicle*. 2021 Materials Today: Proceedings, Department of Mechanical Engineering, Zakir Husain College of Engineering and Technology, Aliagarh Muslim University, <https://doi.org/10.1016/j.matpr.2021.09.247>.
- [11] Ni, J.; Hu, J.; Li, X.; Xu, B.; Zhou, J., *G-G Diagram Generation Based on Phase Plane Method and Experimental Validation for FSAE Race Car*. SAE Technical Papers, April 2016, ISSN: 0148-7191, SAE International, <https://doi.org/10.4271/2016-01-0174>.

- [12] Ozerem, O.; Morrey, Denise, A *brush-based thermo-physical tyre model and its effectiveness in handling simulation of a Formula SAE vehicle*. Proceedings of the Institution of Mechanical Engineers, Part D: Journal of Automobile Engineering, Volume 233, Pages 107-120, January 2019, ISSN: 0954-4070, SAGE Publications Ltd, <https://doi.org/10.1177/0954407018759740>.
- [13] Pacejka, H.B., *Tyre and Vehicle Dynamics*. Oxford, Butterworth-Heinemann, Elsevier Ltd, 2002.
- [14] Russouw, M.; *Development of a Tyre and Vehicle Dynamics Model for Formula SAE*. SAE Technical Papers, Volume 2015-March, 2015, ISSN: 0148-7191, SAE International, <https://doi.org/10.4271/2015-01-0071>.
- [15] Saurabh, Y.S. et al., *Design of Suspension System for Formula Student Race Car*. Procedia Engineering 12th International Conference on Vibration Problems, Volume 144, December 2015, Pages 1138-1149, ISSN: 1877-7058, Elsevier Ltd, <https://doi.org/10.1016/j.proeng.2016.05.081>.
- [16] Schommer, A.; Soliman, P.; Farias, L.T.; Martins, M., *Analysis of a Formula SAE Vehicle Suspension: Chassis Tuning*. SAE Technical Papers, Volume 2015 - September, 2015, ISSN: 0148-7197, SAE International, <https://doi.org/10.4271/2015-36-0275>.
- [17] Sierra, C.; Tseng, E.; Jain, A.; Peng, H., *Cornering stiffness estimation based on vehicle lateral dynamics*. Vehicle System Dynamics, Volume 44, Pages 24-38, 2006, ISSN: 1744-5159, <https://doi.org/10.1080/00423110600867259>.
- [18] Swamy, V.S.; Shivayogi, H.G.K.; Mathivanan, N.R., *Selection of Optimal Tire and Design Optimisation of Steering System for a Formula Student Race Car through Tire Data Treatment*. Journal of Physics: Conference Series, Volume 1478, May 2020, ISSN: 1742-6588, Institute of Physics Publishing, <https://doi.org/10.1088/1742-6596/1478/1/012032>.
- [19] Todoruț, A.; Cordoș, N.; Barabás, I., *Elemente de Dinamica Autovehiculelor*. Cluj-Napoca, Editura U.T.PRESS, 2021.
- [20] Xu, N.; Huang, Y.; Askari, H.; Tang, Z., *Tire Slip Angle Estimation Based on the Intelligent Tire Technology*. IEEE Transactions on Vehicular Technology, Volume 70, Pages 2239-2249, March 2021, ISSN: 0018-9545, Institute of Electrical and Electronics Engineers Inc., <https://doi.org/10.1109/TVT.2021.3059432>.
- [21] Zhang, H.; Zhang, X.; Wang, J., *Robust gain-scheduling energy-to-peak control of vehicle lateral dynamics stabilisation*. Volume 52, Pages 309-340, March 2014, ISSN: 0042-3144, Taylor and Francis Ltd, <https://doi.org/10.1080/00423114.2013.879190>.
- [22] ****Formula SAE Rules VI 2022*, SAE Int., 2021. <https://www.formulastudent.de/fsg/>, (Accessed 22.03.2022).

EVALUAREA COMPARATIVĂ A COMPORTAMENTULUI DINAMIC AL PNEURILOR CARE ECHIPEAZĂ AUTOVEHICULELE DE FORMULA STUDENT, PRIN MODELARE NUMERICĂ

Rezumat: În lucrare sunt surprinse studii privind interacțiunea roată-drum, prin modelarea pneurilor în zona de contact, în cazul autovehiculului de curse din cadrul echipei studențești ART TU Cluj-Napoca, Formula Student Team. Condițiile de drum s-au luat în considerare în conformitate cu circuitul Skidpad din cadrul competiției, iar pentru pneurile luate în studiu s-au considerat diferite presiuni de umflare. Astfel, prin dezvoltarea unui model de calcul numeric în programul MATLAB, cu ajutorul căruia se obțin rezultate comparative, cu interpretare grafică, se pot identifica influențele generate de diferitele pneuri considerate asupra comportamentului dinamic al autovehiculului luat în studiu.

Constantin-Cosmin DANJI, MSc Student, Eng., Technical University of Cluj-Napoca, Faculty of Automotive Engineering, Mechatronics and Mechanics, Department of Automotive Engineering and Transports, Romania, constantincosmin.danci@gmail.com, Office Phone 0264 401 779.

Irina DUMA, PhD Student, Eng., Assistant, Technical University of Cluj-Napoca, Faculty of Automotive Engineering, Mechatronics and Mechanics, Department of Automotive Engineering and Transports, Romania, irina.duma@auto.utcluj.ro, Office Phone 0264 401 779.

Thomas Imre Cyrille BUIDIN, PhD Student, Eng., Assistant, Technical University of Cluj-Napoca, Faculty of Automotive Engineering, Mechatronics and Mechanics, Department of Automotive Engineering and Transports, Romania, Thomas.Buidin@auto.utcluj.ro, Office Phone 0264 401 779.

Nicolae CORDOȘ, PhD. Eng., Associate Professor, Technical University of Cluj-Napoca, Faculty of Automotive Engineering, Mechatronics and Mechanics, Department of Automotive Engineering and Transports, Romania, nicolae.cordos@auto.utcluj.ro, Office Phone 0264 401 779.

Adrian TODORUȚ, PhD. Eng., Professor, Technical University of Cluj-Napoca, Faculty of Automotive Engineering, Mechatronics and Mechanics, Department of Automotive Engineering and Transports, Romania, adrian.todorut@auto.utcluj.ro, Office Phone 0264 401 674.